OncoTargets and Therapy

Dovepress
open access to scientific and medical research

Open Access Full Text Article

ORIGINAL RESEARCH

RETRACTED ARTICLE: Long Noncoding RNA CCDC144NL-AS1 Promotes the Oncogenicity of Osteosarcoma by Acting as a Molecular Sponge for microRNA-490-3p and Thereby Increasing HMGA2 Expression

This article was published in the following Dove Press journal:
OncoTargets and Therapy

Juliang He*
Jian Guan*
Shian Liao
Zhenjie Wu
Bin Liu
Hao Mo
Zhenchao Yuan

Department of Bone and Soft Tissue Surgery, Guangxi Medical University Cancer Hospital, Nanning, Guangxi 530021, People's Republic of China

*These authors contributed equally to this work

Purpose: The long noncoding RNA CCDC144NL antisense RNA 1 (CCDC144NL-AS1) exhibits important functions in gastric cancer. In this study, we aimed to investigate the roles of CCDC144NL-AS1 in modulating the phenotype of osteosarcoma (OS) cells in vitro and in vivo and elucidate its underlying mechanism.

Methods: Reverse transcription quantitative polymerase chain reaction (PCR) was performed to determine the expression level of CCDC144NL-AS1 in OS tissues and cell lines. The proliferation, apoptosis, migration, and invasion in vitro as well as tumor growth in vivo were determined in OS cells using the Cell Counting Kit 8 assay, flow cytometric analysis, transwell migration and invasion assays, and xenograft experiments, respectively. Bioinformatics analysis was performed to identify the potential microRNA targets of CCDC144NL-AS1, which were subsequently confirmed using the luciferase reporter assay, RNA immunoprecipitation assay, reverse transcription quantitative PCR, Western blotting, and rescue experiments.

Results: CCDC144NL-AS1 expression was upregulated in OS tissues and cell lines. Patients with OS who exhibited high CCDC144NL-AS1 expression had shorter overall survival than those who exhibited low CCDC144NL-AS1 expression. Functionally, interference in CCDC144NL-AS1 expression led to a notable decrease in the proliferation, migration, and invasion of OS cells and an increase in cell apoptosis in vitro. Furthermore, CCDC144NL-AS1 knockdown impaired OS tumor growth in vivo. Mechanistically, CCDC144NL-AS1 directly bound to miR-490-3p in OS cells, where it functioned as a molecular sponge and subsequently increased the expression of high-mobility group AT-hook 2 (HMGA2). Rescue experiments further demonstrated that miR-490-3p suppression or HMGA2 restoration abated CCDC144NL-AS1 deficiency-induced cancer-inhibitory actions in OS cells.

Conclusion: CCDC144NL-AS1 exhibits pro-oncogenic roles in OS by functioning as a sponge for miR-490-3p and increasing HMGA2 expression. Our findings suggest that greater understanding of the CCDC144NL-AS1/miR-490-3p/HMGA2 pathway can provide useful information for OS diagnosis, prognosis, and therapy.

Keywords: long noncoding RNA, microRNA, competitive endogenous RNA, high-mobility group AT-hook 2

Introduction

Osteosarcoma (OS) is the most common and most aggressive type of bone tumor originating from bone marrow mesenchymal stem cells.[1] OS mainly occurs in young people, with a peak incidence at 14–20 years.[2] The annual incidence of

Correspondence: Hao Mo; Zhenchao Yuan
Email mohaogxzlyy@163.com; yzccwhyzw@163.com

submit your manuscript | www.dovepress.com
DovePress
http://doi.org/10.2147/OTT.S280912

OS is approximately 4.5 per million people.[3] At present, the major treatment strategies for OS are surgery and radiochemotherapy.[4] Improved therapeutic techniques and perioperative management have led to considerable advances in the development of diagnostic methods. As a result, the prognosis of OS has considerably increased in the last decade.[5] Despite this, the clinical efficacy of patients with advanced-stage OS remains unsatisfactory, with a 5-year survival rate of only 30%–40%.[6] The poor prognosis of OS is considered to be due to the recurrence and metastasis of the disease.[7] Therefore, there is a desperate need to unveil the key mechanisms associated with OS oncogenesis and progression in order to identify attractive treatment strategies against OS.

Long noncoding RNAs (lncRNAs) are a group of noncoding transcripts that are more than 200 nucleotides in length.[8] Although they are incapable of encoding proteins, lncRNAs can regulate gene expression via multiple mechanisms, including direct interaction with mRNAs, microRNAs (miRNAs), circular RNAs, and proteins.[9] lncRNAs are implicated in the regulation of various cellular processes, including cellular signal transduction, chromosome imprinting, hormonal control, and genetic translation; therefore, the dysregulation of lncRNAs can result in several diseases, including cancer.[10] Changes in lncRNA expression have been frequently observed in patients with OS, in which lncRNAs function as tumor promoters or inhibitors to control a variety of malignant processes.[11,12]

miRNAs are a set of highly conserved, single-stranded, and noncoding RNA transcripts that are 18–24 nucleotides in length.[13] They can modulate gene expression at the post-transcriptional level by directly binding to the 3′-untranslated regions (3′UTRs) of their target mRNAs and triggering translational repression or mRNA impairment.[14] The differential expression of miRNAs is closely related to OS malignancy.[15] Increasing evidence suggests that lncRNAs play antitumor or tumor-promoting roles in OS progression.[16–18] Recently, the competitive endogenous RNA (ceRNA) hypothesis was developed, which suggests that there is a regulatory network comprising lncRNAs, miRNAs, and mRNAs.[19] lncRNAs can function as ceRNAs for certain miRNAs and thereby enhance target mRNA expression.[19] Therefore, exploring the lncRNA/miRNA axis may provide useful information for OS clinical diagnosis and therapy.

The lncRNA DCST1 antisense RNA 1 (CCDC144NL-AS1) has been shown to play important roles in cancer progression in gastric cancer.[20] However, its expression status, specific roles, and working mechanism in OS remain poorly understood. Accordingly, in this study, we aimed to investigate the roles of CCDC144NL-AS1 in modulating the phenotype of OS cells in vitro and in vivo and elucidate its underlying mechanisms. Our results may improve our understanding regarding the mechanisms underlying OS pathogenesis and help develop promising targets for cancer diagnosis, prognosis, and therapy.

Materials and Methods

Tissue Samples and Cell Lines

This study was approved by the Institutional Ethics Review Board of Guangxi Medical University Cancer Hospital (GXMUCH.2016[illegible]0216) and conducted in accordance with the Declaration of Helsinki. Written informed consent for the use of tissues was obtained from all subjects. Fifty-seven pairs of OS tissues and matched adjacent normal bone tissues were collected from patients admitted to Guangxi Medical University Cancer Hospital. No patient had received any antitumor therapies prior to their enrollment in this study. The collected tissue specimens were quickly frozen in liquid nitrogen after tissue resection and preserved in liquid nitrogen until future use.

The normal human osteoblast cell line hFOB1.19 and three OS cell lines U-2OS, HOS, and Saos-2 were obtained from the Institute of Biochemistry and Cell Biology of the Chinese Academy of Sciences (Shanghai, China). hFOB1.19 cells were cultured in a medium containing Dulbecco's modified Eagle medium and Nutrient Mixture F-12 supplemented with 0.3 mg/mL G418 and 10% fetal bovine serum (FBS; all from Gibco; Thermo Fisher Scientific, Inc., Waltham, MA, USA). The cell lines HOS and U-2OS were maintained in minimum essential a (Gibco; Thermo Fisher Scientific, Inc.) and McCoy's 5a Medium (Gibco; Thermo Fisher Scientific, Inc.), respectively, both of which were supplemented with 10% FBS. McCoy's 5a Medium plus 15% FBS was used to culture Saos-2 cells. The OS cell line 143B was obtained from American Type Culture Collection (Manassas, VA, USA) and was grown in minimum essential medium supplemented with 10% FBS. All cells were maintained at 37°C in a 5% CO_2 incubator.

Cell Transfection

Small interfering RNAs (siRNAs) targeting CCDC144NL-AS1 (si-CCDC144NL-AS1, including si-CCDC144NL-AS1#1, si-CCDC144NL-AS1#2, and si-CCDC144NL-AS1#3), negative control siRNA (si-NC), miR-490-3p mimic, miRNA mimic NC (miR-NC), miR-490-3p inhibitor (anti-miR-490-3p), and negative NC (anti-NC) were purchased from Shanghai GenePharma Co., Ltd. (Shanghai, China). The HMGA2 overexpression plasmid pcDNA3.1-HMGA2 (pc-HMGA2) and control empty pcDNA3.1 plasmid were synthesized by Guangzhou RiboBio Co., Ltd. (Guangzhou, China). Cells were seeded into 6-well plates, followed by the transfection of the above-mentioned oligonucleotides and plasmids using the Lipofectamine™ 2000 transfection reagent (Thermo Fisher Scientific).

Subcellular Fractionation Assay

The Cytoplasmic and Nuclear RNA Purification Kit (Norgen Biotek, Thorold, Canada) was used to separate and purify the cytoplasmic and nuclear RNA fractions in OS cells.

RNA Isolation and Reverse Transcription Quantitative Polymerase Chain Reaction (RT-qPCR) Analysis

Total RNA was extracted from tissues or cells using TRIzol (Invitrogen; Thermo Fisher Scientific, Inc.), and the concentration and purity of total RNA were determined using the Nanodrop 2000 spectrophotometer (Invitrogen; Thermo Fisher Scientific). Total RNA was reverse-transcribed into cDNA using the FastKing RT Kit (TIANGEN, Beijing, China). Then, the expression levels of CCDC144NL-AS1 and HMGA2 were determined by quantitative PCR using the Quant One-Step qRT-PCR Kit (TIANGEN). GAPDH served as the internal reference for CCDC144NL-AS1 and HMGA2 expression. To quantify miR-490-3p expression, cDNA was synthesized using the miRcute miRNA cDNA First-Strand Synthesis Kit (TIANGEN) and then subjected to quantitative PCR using the miRcute Enhanced miRNA qPCR Kit (TIANGEN). The expression level of miR-490-3p was normalized to that of U6 small nuclear RNA. All data were analyzed using the threshold cycle $2^{-\Delta\Delta Ct}$ method.

Cell Counting Kit 8 (CCK-8) Assay

After 24 h of cultivation, the transfected cells were collected and reseeded into 96-well plates at a density of 2000 cells/well. The CCK-8 assay (Dojindo Molecular Technologies, Inc., Kumamoto, Japan) was performed every 24 h to monitor cell proliferation. Cells were treated with 10 μL of the CCK-8 reagent for 2 h. The absorbance was measured at a wavelength of 450 nm using a microplate reader (Bio-Rad Laboratories, Benicia, CA, USA).

Flow Cytometric Analysis

Cell apoptosis was detected using the Annexin V-fluorescein isothiocyanate (FITC) Apoptosis Detection Kit (BioLegend, San Diego, CA, USA). Briefly, 0.25% EDTA-free trypsin was used to harvest the transfected cells at 48 h after transfection. The transfected cells were rinsed with phosphate-buffered saline at 4°C. Following centrifugation at 4°C, phosphate-buffered saline was discarded, the collected cells were resuspended in 100 μL of binding buffer and then 5 μL of annexin V–FITC and 5 μL of propidium iodide were added. The apoptosis rate was analyzed using a flow cytometer (FACScan; BD Biosciences, Franklin Lakes, NJ, USA) using the CellQuest software (BD Biosciences).

Transwell Migration and Invasion Assays

Transfected cells were collected after 48 h of culture and resuspended in FBS-free culture medium with the cell density adjusted to 3×10^5 cells/mL. For migration assays, the upper compartments of the Transwell inserts (pore diameter: 8 μm; BD Biosciences) were covered with 100 μL of the cell suspension. Culture medium (500 μL) supplemented with 20% FBS was added to the lower compartments. The transfected cells were cultured at 37°C with 5% CO_2 for 24 h. Then, the nonmigrated cells on the surface of the upper chamber were gently removed using a cotton bud, whereas the migrated cells were fixed with 4% paraformaldehyde and stained with 0.5% crystal violet. The number of migrated cells in five randomly chosen visual fields was counted under an inverted microscope (Olympus, Tokyo, Japan). Matrigel (BD Biosciences)-coated Transwell chambers were used for the invasion assays; all other procedures were similar to those used in the migration assay.

Xenograft Experiment

Lentiviral vectors carrying short hairpin RNA (shRNA) specifically targeting CCDC144NL-AS1 (sh-CCDC144NL-AS1) or negative control shRNA (sh-NC) were designed and chemically synthesized by Shanghai GenePharma Co., Ltd. HOS cells were transfected with the lentiviral vectors, and puromycin was used to select the stable CCDC144NL-AS1 knockdown cell line. Male BALB/c nude mice aged 4–6 weeks were obtained from Hunan SJA Laboratory Animal Co., Ltd. (Changsha, Hunan). All experiments involving animals were performed under the approval of the Animal Experimental Ethics Committee of Guangxi Medical University Cancer Hospital (GXMUCH.2019-0411) and conducted in accordance with the NIH guidelines for the care and use of laboratory animals. A 100-μL cell suspension containing 2×10^6 sh-CCDC144NL-AS1 or sh-NC stably transfected HOS cells was subcutaneously inoculated into nude mice. One week after the inoculation, the length and width of tumor xenografts were measured every 4 days using a Vernier caliper. Tumor volume was determined using the following equation: volume (mm^3) = 0.5 × length × $width^2$. All mice were euthanized at 31 days after cell injection; tumor xenografts were dissected, weighed, and stored at –80°C until further use.

Immunohistochemical (IHC) Analysis

Tumor xenografts were fixed with 4% neutral formalin and embedded in paraffin. The paffin-embedded samples were cut into 4-μm-thick sections, deparaffinized using xylene, and then rehydrated using a gradient ethanol gradient. After culturing the samples with 0.3% H_2O_2 for 30 min and blocking with 5% bovine serum albumin (R&D Systems) for 45 min at 37°C, the sections were probed with HMGA2 (cat. no. ab97301; Abcam, Cambridge, MA, USA) at 4°C overnight. Next, a horseradish peroxidase-conjugated secondary antibody (cat. no. ab205718; Abcam) was used as the secondary antibody. The section were then incubated at room temperature for 45 min. Finally, the sections were stained with 3,3′-diaminobenzidine, counterstained with hematoxylin, and then dehydrated using ethanol. Images were acquired using an Olympus inverted microscope.

Bioinformatics Analysis

Data for 262 patients with sarcoma were downloaded from The Cancer Genome Atlas (TCGA; https://portal.gdc.cancer.gov/) database, a large-scale cancer research project, and the CCDC144NL-AS1 expression data (262 tumor tissues and 2 adjacent normal tissues) were extracted.

StarBase 3.0 (http://starbase.sysu.edu.cn/) and miRcode (http://www.mircode.org/) were used to identify the potential miRNAs targeting CCDC144NL-AS1.

RNA Immunoprecipitation (RIP) Assay

The RIP assay was performed using the Magna RIP RNA-Binding Protein Immunoprecipitation Kit (Merck Millipore, Darmstadt, Germany). OS cells were harvested and lysed with RIP lysis buffer (Beyotime Biotechnology Co.; Shanghai, China). Following centrifugation, the supernatant was collected and 10% of the cell lysate was used as the "input." The residual cell lysate was incubated overnight at 4°C with magnetic beads conjugated with human anti-argonaute 2 (Ago2; Millipore) or anti-immunoglobulin G (IgG; Millipore) antibodies. The immunoprecipitated RNA was extracted and reverse-transcribed into cDNA. The synthesized cDNA was used as a template, and RT-qPCR was conducted to detect the expression of CCDC144NL-AS1 and miR-490-3p.

Luciferase Reporter Assay

The fragments of CCDC144NL-AS1 that contained wild-type predicted wild-type (WT) miR-490-3p binding site and mutant (MUT) CCDC144NL-AS1 fragments were amplified and inserted into the pmirGLO luciferase reporter plasmid (Promega Corporation, Madison, WI, USA) to generate WT-CCDC144NL-AS1 and MUT-CCDC144NL-AS1, respectively. The same experimental steps were used to synthesize WT-HMGA2 and MUT-HMGA2. Cells were seeded into 6-well plates and transfected with the constructed WT or MUT reporter plasmids together with miR-490-3p mimic or miR-NC using Lipofectamine 2000. After 48 h of incubation, luciferase activity was determined using the Dual-Luciferase Assay System (Promega) and normalized to Renilla luciferase activity.

Western Blotting

Using RIPA buffer (Solarbio, Shanghai, China), total protein was extracted from the transfected cells. After quantification with the BCA Protein Assay Kit (Beyotime Biotechnology), total proteins were separated via 10% sodium dodecyl sulfate-polyacrylamide gel electrophoresis and transferred on to polyvinylidene fluoride blotting membranes. The membranes were then blocked with 5% nonfat milk at room temperature for 2 h and then incubated overnight at 4°C

with primary antibodies against HMGA2 (ab246513; Abcam, Cambridge, MA, USA) or GAPDH (ab181603; Abcam). The membranes were incubated with horseradish peroxidase-conjugated secondary antibody (ab6721; Abcam) at room temperature for 2 h. The ECL Advance Western Blotting Detection Kit (GE Healthcare, Amersham, UK) was used to visualize protein signals.

Statistical Analysis

All results are expressed as mean ± standard deviation from at least three independent experiments. Comparisons between the two groups were conducted using the Student's *t*-test, whereas a one-way analysis of variance along with Tukey's post hoc test was used to analyze the differences among multiple groups. The correlation between CCDC144NL-AS1 and miR-490-3p expression in OS tissues was determined using Pearson's correlation coefficient. $P < 0.05$ was considered statistically significant.

Results

Loss of CCDC144NL-AS1 Inhibits the Malignant Characteristics of OS Cells in vitro

Initially, CCDC144NL-AS1 expression status was analyzed in OS cells using the TCGA database. High CCDC144NL-AS1 expression was observed in OS tissues than in normal tissues (Figure 1A). To confirm this observation, CCDC144NL-AS1 expression in 57 pairs of OS tissues and matched adjacent normal tissues was analyzed using RT-qPCR. Consistently, CCDC144NL-AS1 was overexpressed in OS tissues than in normal tissues (Figure 1B). Additionally, all four OS cell lines (HOS, U-2OS, 143B, and Saos-2) showed relatively higher CCDC144NL-AS1 expression than the normal human osteoblast hFOB1.19 cell line (Figure 1C). Furthermore, overall survival was shorter in OS patients with high CCDC144NL-AS1 expression than in those with low CCDC144NL-AS1 expression (Figure 1D).

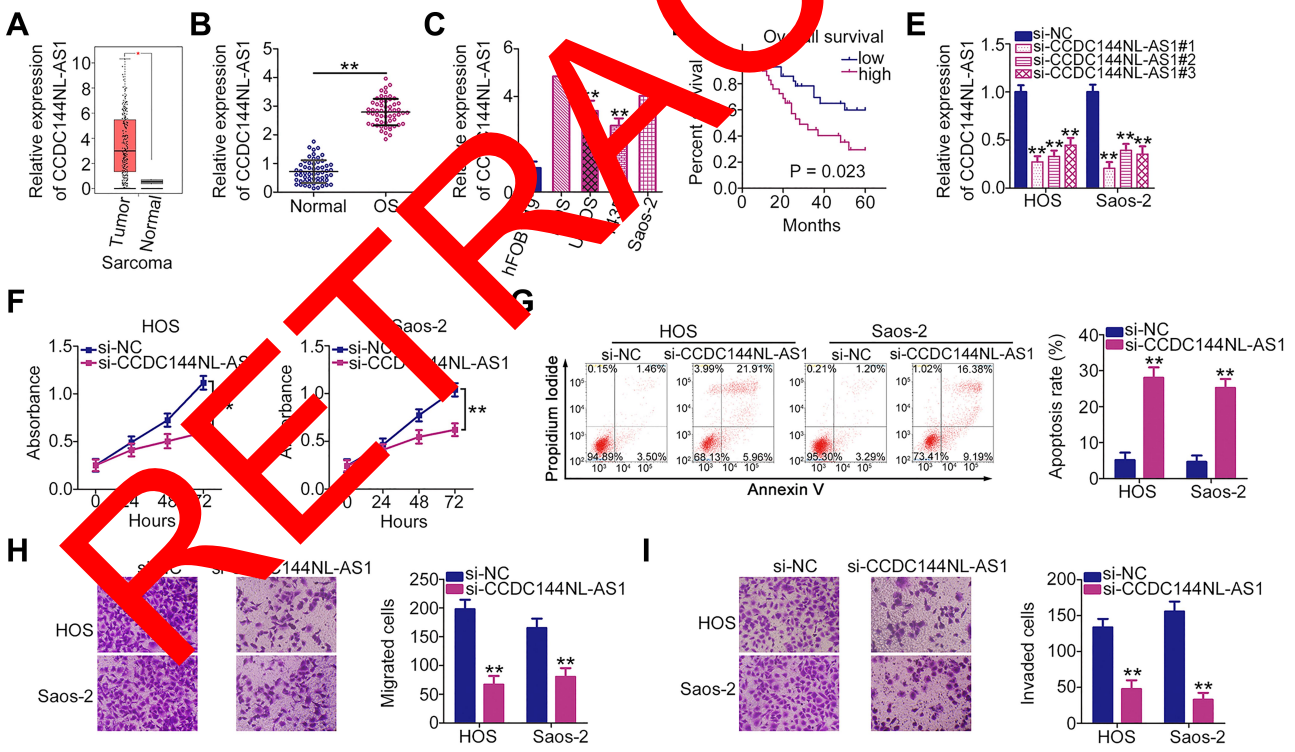

Figure 1 Long noncoding RNA DCST1 antisense RNA 1 (CCDC144NL-AS1) knockdown inhibits the proliferation, migration, and invasion of osteosarcoma (OS) cells and promotes cell apoptosis in vitro. (**A**) The Cancer Genome Atlas (TCGA) database was used to analyze the expression profile of CCDC144NL-AS1 in OS cells. (**B**) Reverse transcription quantitative polymerase chain reaction (RT-qPCR) was used to determine the relative expression level of CCDC144NL-AS1 in 57 pairs of OS tissues and corresponding adjacent normal tissues. (**C**) Expression of CCDC144NL-AS1 in OS cell lines (HOS, U-2OS, 143B, and Saos-2) and the normal human osteoblast hFOB1.19 cell line was measured via RT-qPCR. (**D**) Overall survival curve according to CCDC144NL-AS1 expression in patients with OS. (**E**) RT-qPCR analysis was used to assess the efficiency of si-CCDC144NL-AS1 transfection. (**F**) Cell proliferation ability of HOS and Saos-2 cells transfected with si-CCDC144NL-AS1 or si-NC was detected via the Cell Counting Kit 8 (CCK-8) assay. (**G**) Flow cytometry was used to analyze the apoptosis rate of HOS and Saos-2 cells after CCDC144NL-AS1 depletion. (**H** and **I**) The effects of CCDC144NL-AS1 knockdown on the migration and invasion of HOS and Saos-2 cells were evaluated by Transwell migration and invasion assays. **P < 0.01.

HOS and Saos-2 cell lines, which showed the highest endogenous CCDC144NL-AS1 expression among the four OS cell lines, were transected with si-CCDC144NL-AS1 to knockdown endogenous CCDC144NL-AS1. The transfection efficiency was confirmed using RT-qPCR (Figure 1E). Given its relatively high silencing efficiency, si-CCDC144NL-AS1#1 was selected for subsequent functional assays. CCDC144NL-AS1 downregulation evidently suppressed the proliferation of HOS and Saos-2 cells, as revealed by the CCK-8 assay (Figure 1F). In addition, the apoptosis rate was substantially increased following CCDC144NL-AS1 depletion (Figure 1G). Furthermore, the effects of CCDC144NL-AS1 knockdown on the migration and invasion of OS cells were determined using Transwell migration and invasion assays: CCDC144NL-AS1 loss impaired the migration (Figure 1H) and invasive (Figure 1I) abilities of HOS and Saos-2 cells. Taken together, these results demonstrate the cancer-promoting role of CCDC144NL-AS1 in OS cells.

CCDC144NL-AS1 Functions as a Molecular Sponge for miR-490-3p in OS Cells

The subcellular localization of CCDC144NL-AS1 was predicted by lncATLAS (http://lncatlas.crg.eu/) and lncLocator (http://www.csbio.sjtu.edu.cn/bioinf/lncLocator/) to determine the mechanisms by which CCDC144NL-AS1 exerts its oncogenic actions in OS cells. CCDC144NL-AS1 was predicted to be a cytoplasmic lncRNA (Figure 2A and B). Subcellular fractionation was performed to assess its distribution in OS cells. The results demonstrated that CCDC144NL-AS1 was most abundant in the cytoplasm of HOS and Saos-2 cells (Figure 2C). This suggests that CCDC144NL-AS1 may act as a molecular sponge or ceRNA for miRNAs to modulate gene expression at the post-transcriptional level. Using online databases that decipher lncRNA–miRNA interactions (StarBase version 3.0 and miRcode), six miRNAs (miR-145-5p, miR-29a-3p, miR-29b-3p, miR-29c-3p, miR-29d-3p, and miR-490-3p) were found to possess complementary sequence pairing with CCDC144NL-AS1 (Figure 2D).

RT-qPCR was performed to explore the ability of CCDC144NL-AS1 to regulate the expression of these candidates in OS cells. The results showed that CCDC144NL-AS1 knockdown notably upregulated miR-490-3p expression in HOS and Saos-2 cells, whereas the expression of the other five miRNAs remained unchanged (Figure 2E). Additionally, miR-490-3p was downregulated in OS tissues (Figure 2F), which inversely correlated with CCDC144NL-AS1 expression (Figure 2G; $r = -0.5716$, $P < 0.0001$). The WT and mutant binding sites of miR-490-3p within CCDC144NL-AS1 are presented in Figure 2H. The luciferase reporter assay was used to examine whether CCDC144NL-AS1 can directly bind to miR-490-3p in OS cells. A miR-490-3p mimic was used in this assay, and its transfection efficiency was evaluated using RT-qPCR. Transfection with the miR-490-3p mimic clearly increased miR-490-3p expression in HOS and Saos-2 cells (Figure 2I). The luciferase reporter assay showed that the luciferase activity of WT-CCDC144NL-AS1 was dramatically decreased following the upregulation of miR-490-3p in HOS and Saos-2 cells, which was abrogated in cells transfected with MUT-CCDC144NL-AS1 (Figure 2J). In addition, CCDC144NL-AS1 and miR-490-3p were enriched in Ago2-containing beads compared with than in control IgG-containing beads (Figure 2K). These results suggest that CCDC144NL-AS1 functions as a molecular sponge for miR-490-3p in OS cells.

HMGA2 is a Direct Target Gene of miR-490-3p in OS Cells

Next, the detailed roles of miR-490-3p in the oncogenicity of OS cells were determined. Ectopic miR-490-3p expression obviously suppressed HOS and Saos-2 cell proliferation (Figure 3A) and induced apoptosis (Figure 3B), as demonstrated by the CCK-8 assay and flow cytometric analysis. In addition, the migration and invasion of HOS and Saos-2 cells after miR-490-3p mimic or miR-NC transfection were assessed using Transwell migration and invasion assays. The results revealed that miR-490-3p-overexpressing HOS and Saos-2 cells showed both impaired migration (Figure 3C) and invasive (Figure 3D) abilities compared with the miR-NC group.

HMGA2 (Figure 3E) was previously identified as a direct target of miR-490-3p in OS cells.[21] Additionally, it is known to play critical roles in OS genesis and progression.[22,23] To confirm these findings, the luciferase reporter assay was performed to detect the binding of miR-490-3p to the 3′-UTR of HMGA2. The luciferase activity of WT-HMGA2 was downregulated by miR-490-3p overexpression in HOS and Saos-2 cells, whereas MUT-HMGA2 activity was unaltered in response to miR-490-3p mimic cotransfection (Figure 3F). Additionally, RT-qPCR and Western blotting confirmed that miR-490-3p overexpression led to a significant decrease in the mRNA (Figure 3G) and protein (Figure 3H) expression levels

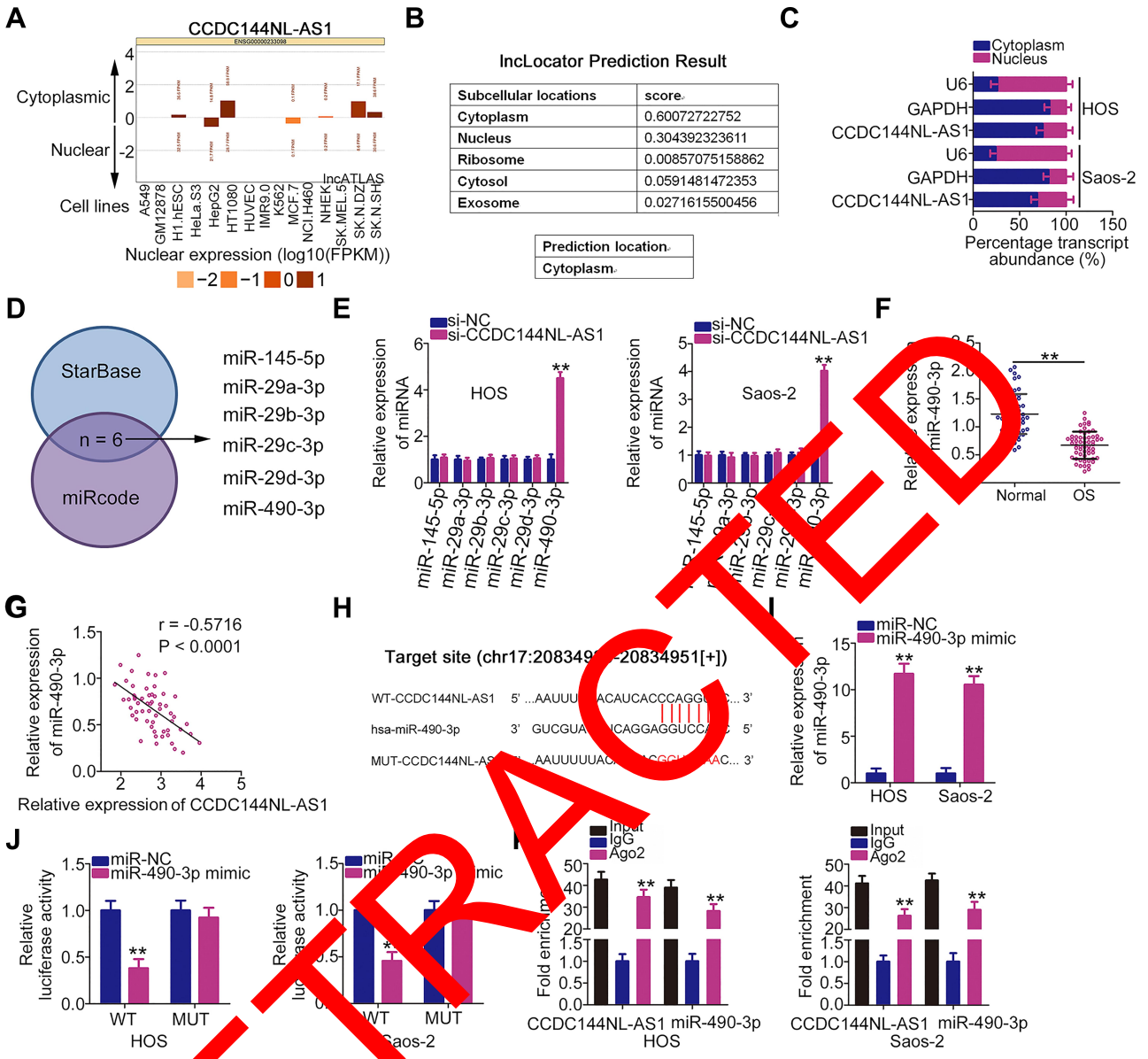

Figure 2 Long noncodi NA DCST ntisense RNA 1 (CCDC144NL-AS1) acts as a molecular sponge for miR-490-3p in osteosarcoma (OS) cells. (**A** and **B**) lncRNA subcellular localization pre ors LATLAS an lncLocator were used to predict CCDC144NL-AS1 localization. (**C**) Subcellular fractionation assay showed that CCDC144NL-AS1 mostly ated in the toplasm of HOS and Saos-2 cells. (**D**) StarBase 3.0 and miRcode were used to identify the putative miRNAs targeting CCDC144NL-A . (**E**) verse tr cripti quantitative polymerase chain reaction (RT-qPCR) was used to measure the mRNA expression in CCDC144NL-AS1-depleted HOS and S -2 cells. RT-qPCR sis was conducted to measure miR-490-3p expression in 57 pairs of OS tissues and adjacent normal tissues. (**G**) Pearson's correlati oefficient owed the relationship between miR-490-3p and CCDC144NL-AS1 in the 57 OS tissues. (**H**) The wild-type and mutant miR-490-3p binding sequences i CC re shown. (**I**) HOS and Saos-2 cells were transfected with miR-490-3p mimic or miR-NC, and RT-qPCR was performed to assess the transfection ef cy. (**J**) Luciferase reporter assay demonstrated the binding of miR-490-3p to CCDC144NL-AS1 in OS cells. (**K**) RNA immunoprecipitation (RIP) assay was performed to termine the interaction between miR-490-3p and CCDC144NL-AS1 in OS cells. **P < 0.01.

of HMGA2 in HOS and Saos-2 cells. Furthermore, the mRNA expression levels of HMGA2 were higher in OS tissues than in matched adjacent normal tissues (Figure 3I). Pearson's correlation coefficient showed that there was an inverse correlation between miR-490-3p and HMGA2 mRNA expression levels in the 57 OS tissues (Figure 3J; r = –0.6227, P < 0.0001). These results demonstrate that HMGA2 is a direct target of miR-490-3p in OS cells.

The CCDC144NL-AS1/miR-490-3p/HMGA2 Pathway is Implicated in OS Progression

As CCDC144NL-AS1 functions as a molecular sponge for miR-490-3p, we next determined whether HMGA2 was regulated by CCDC144NL-AS1 in OS cells via miR-490-3p sponging. Depleted CCDC144NL-AS1 expression obviously suppressed

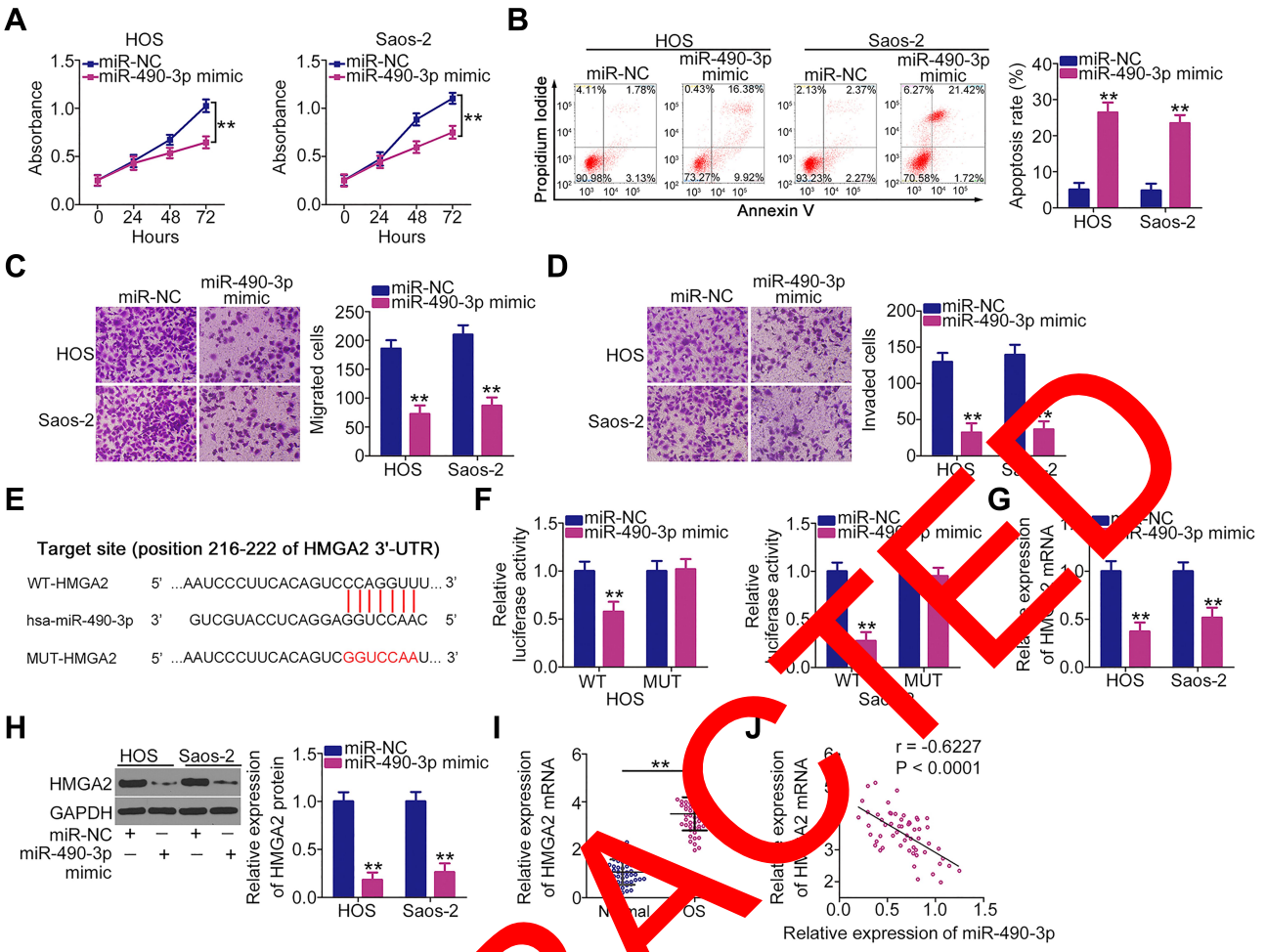

Figure 3 High-mobility group AT-hook 2 (HMGA2) is a direct target of miR-490-3p in osteosarcoma (OS) cells. (**A** and **B**) Cell Counting Kit 8 (CCK-8) assay and flow cytometric analysis were performed to investigate the proliferation and apoptosis of HOS and Saos-2 cells after miR-490-3p mimic or miR-NC injection. (**C** and **D**) Migration and invasion of miR-490-3p mimic-transfected or miR-NC-transfected HOS and Saos-2 cells were evaluated using Transwell migration and invasion assays. (**E**) Scheme showing the sequences of wild-type and mutant miR-490-3p binding sites in the 3′-untranslated region (UTR) of HMGA2. (**F**) Luciferase activity was detected in HOS and Saos-2 cells after cotransfection with miR-490-3p mimic or miR-NC and WT-HMGA2 or MUT-HMGA2. (**G** and **H**) HOS and Saos-2 cells transfected with miR-490-3p mimic or miR-NC were analyzed via reverse transcription quantitative polymerase chain reaction (RT-qPCR) and Western blotting to quantify HMGA2 mRNA and protein levels. (**I**) mRNA expression levels of HMGA2were detected in 57 pairs of OS tissues and adjacent normal tissues by RT-qPCR. (**J**) Inverse correlation between HMGA2 mRNA and miR-490-3p in the 57 OS tissues was verified by Pearson's correlation coefficient. **P < 0.01.

the mRNA (Figure 4A) and protein (Figure 4B) expression levels of HMGA2 in HOS and Saos-2 cells. Notably, CCDC144NL-AS1 expression positively correlated with the mRNA expression levels of HMGA2 in the 57 OS tissues (Figure 4C; r = 0.6048, P < 0.0001). Furthermore, the RIP assay confirmed that CCDC144NL-AS1, miR-490-3p, and HMGA2 were all enriched by Ago2 antibody precipitation (Figure 4D), implying that CCDC144NL-AS1, miR-490-3p, and HMGA2 coexist in an RNA-induced silencing complex. Next si-CCDC144NL-AS1 in combination with miR-490-3p inhibitor (anti-miR-490-3p) or NC inhibitor (anti-NC) were transfected into HOS and Saos-2 cells, CCDC144NL-AS1-deficiency resulted in the downregulation of the mRNA (Figure 4E) and protein (Figure 4F) expression of HMGA2, whereas the regulatory actions were abolished by miR-490-3p inhibition.

Rescue experiments were performed to confirm whether the miR-490-3p/HMGA2 pathway is necessary for the tumor-promoting actions of CCDC144NL-AS1 in OS cells. First, the transfection efficiency of anti-miR-490-3p was determined by RT-qPCR (Figure 5A). Transfection with anti-miR-490-3p resulted in a significant decrease in miR-490-3p expression in HOS and Saos-2 cells. The CCK-8 assay and flow cytometric analysis revealed that decreased CCDC144NL-AS1 expression inhibited HOS and Saos-2 cell proliferation (Figure 5B) and promoted cell apoptosis (Figure 5C), whereas anti-miR-490-3p

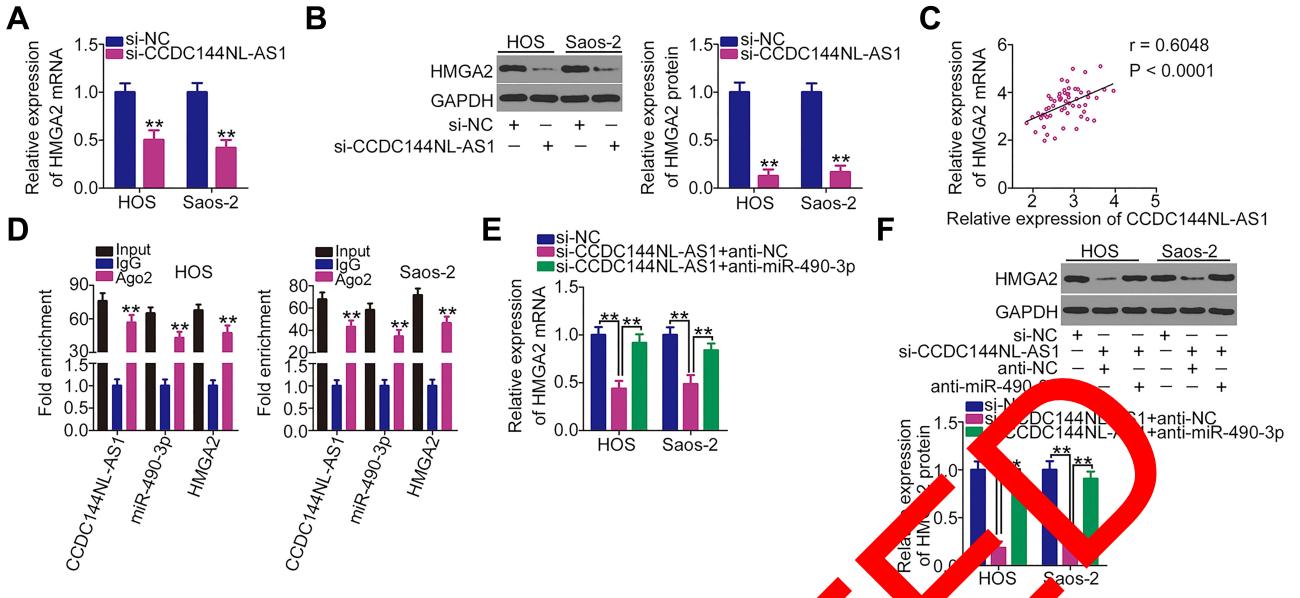

Figure 4 Long noncoding RNA DCST1 antisense RNA 1 (CCDC144NL-AS1) regulates high-mobility group AT-hook 2 (HMGA2) expression in OS cells by decoying miR-490-3p. (**A** and **B**) mRNA and protein expression levels of HMGA2 in HOS and Saos-2 cells after CCDC144NL-AS1 or sh-NC transfection were detected via reverse transcription quantitative polymerase chain reaction (RT-qPCR) and Western blotting, respectively. (**C**) Relationship between HMGA2 mRNA and CCDC144NL-AS1 in the 57 OS tissues was examined according to Pearson's correlation coefficient. (**D**) RNA immunoprecipitation (RIP) assay was performed to assess the interaction between CCDC144NL-AS1, miR-490-3p, and HMGA2 in OS cells. (**E** and **F**) mRNA and protein expression levels of HMGA2 were measured in CCDC144NL-AS1-downregulated HOS and Saos-2 cells after cotransfection with anti-miR-490-3p or anti-NC. **P < 0.01

cotransfection abolished these effects. Additionally, the inhibitory effects of CCDC144NL-AS1 knockdown on HOS and Saos-2 cell migration (Figure 5D) and invasion (Figure 5E) were restored by cotransfection with anti-miR-490-3p.

Further rescue experiments were performed in HOS and Saos-2 cells by cotransfecting si-CCDC144NL-AS1 with the HMGA2 overexpression plasmid pcDNA3.1-HMGA2 (pc-HMGA2) or an empty pcDNA3.1 plasmid. Western blotting confirmed that pcDNA3.1-HMGA2 increased the protein expression level of HMGA2 in HOS and Saos-2 cells (Figure 6A). Functionally, the CCDC144NL-AS1 knockdown-mediated effects on HOS and Saos-2 cell proliferation (Figure 6B), apoptosis (Figure 6C), migration (Figure 6D), and invasion (Figure 6E) were neutralized after cotransfection with pcDNA3.1-HMGA2. Collectively, these results indicate that CCDC144NL-AS1 exhibits tumor-promoting activities in OS cells by regulating the miR-490-3p/HMGA2 axis.

CCDC144NL-AS1 Inhibition Alleviates OS Tumor Growth in vivo

A xenograft experiment was performed to determine whether CCDC144NL-AS1 knockdown suppresses OS tumor growth in vivo. HOS cells stably expressing sh-CCDC144NL-AS1 or sh-NC via lentiviral infection were subcutaneously injected into nude mice. The growth of tumor xenografts was evidently slower in the sh-CCDC144NL-AS1 group than in the sh-NC group (Figure 7A and B). In addition, tumor xenografts derived from CCDC144NL-AS1-depleted HOS cells weighed less than those collected from sh-NC cells (Figure 7C). Total RNA and protein were extracted from tumor xenografts and used to detect CCDC144NL-AS1, miR-490-3p, and HMGA2: in tumor xenografts originating from sh-CCDC144NL-AS1 stably transfected HOS cells, CCDC144NL-AS1 (Figure 7D) and HMGA2 protein (Figure 7E) expression obviously decreased, whereas miR-490-3p (Figure 7F) expression increased. Furthermore, IHC analysis was performed to detect HMGA2 expression in tumor xenografts. The data revealed that HMGA2 expression was downregulated in CCDC144NL-AS1-silenced tumor xenografts (Figure 7G). Taken together, these results reveal the inhibitory effect of CCDC144NL-AS1 silencing on OS tumor growth in vivo.

Discussion

Recently, the multifaceted biological roles of lncRNAs in OS oncogenesis and progression have been uncovered.[24,25] Differentially expressed lncRNAs are implicated in the regulation of gene transcription, post-transcriptional

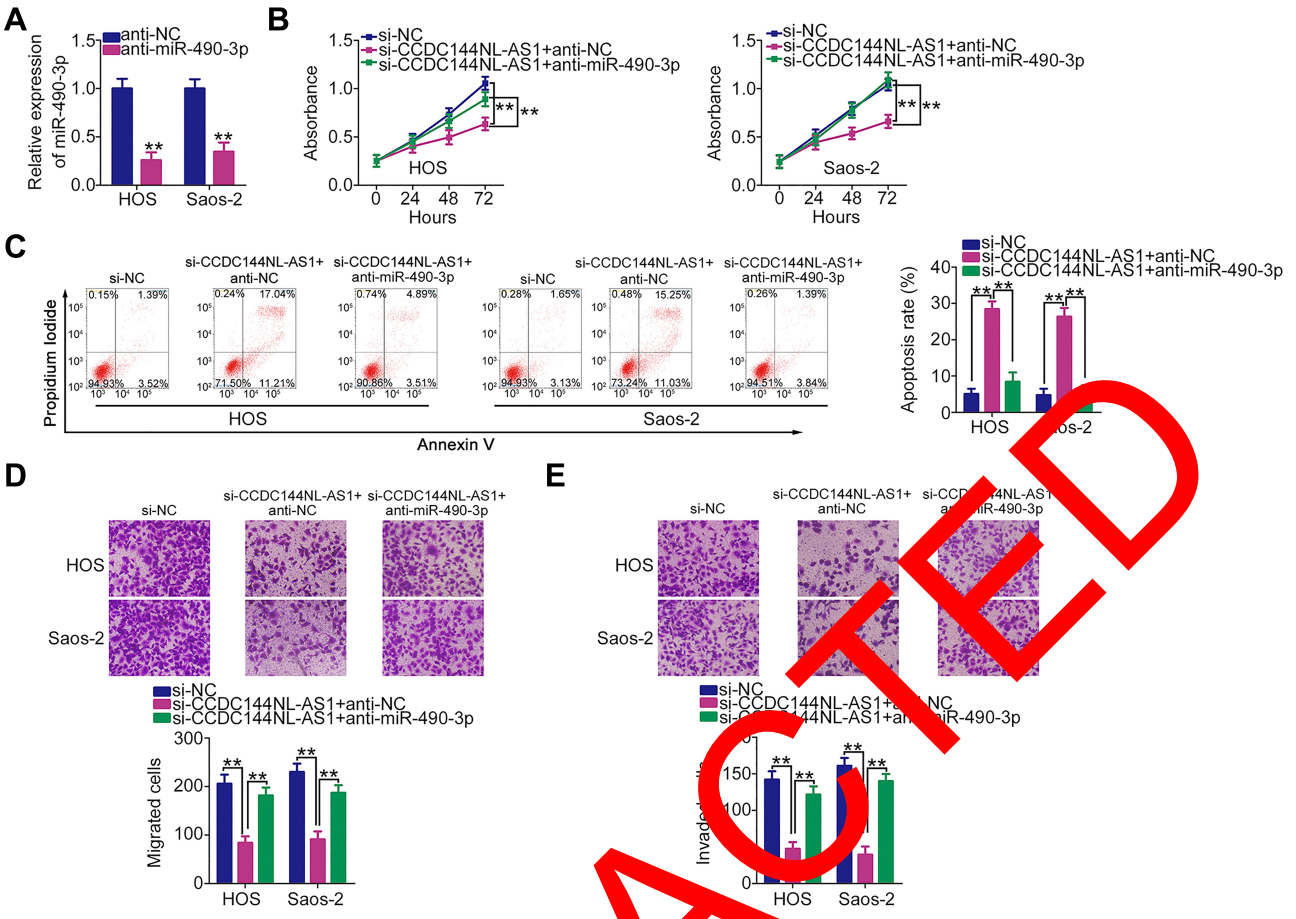

Figure 5 miR-490-3p Inhibition abrogates the tumor-suppressing e[illegible] of long nc[illegible]ing RNA DCST1 antisense RNA 1 (CCDC144NL-AS1) knockdown in HOS and Saos-2 cells. (**A**) HOS and Saos-2 cells were transfected with [illegible]ti-miR[illegible]0-3p or [illegible]ti-NC, and the transfection efficiency was determined via reverse transcription quantitative polymerase chain reaction (RT-qPCR). (**B–E**) si-C[illegible]C144NL-[illegible]1 together[illegible]ith anti-miR-490-3p or anti-NC was cotransfected into HOS and Saos-2 cells. The Cell Counting Kit 8 (CCK-8) assay, flow cytometric analy[illegible] and Tra[illegible]ration and invasion assays were performed to determine cell proliferation, apoptosis, migration, and invasion, respectively. **P < 0.01.

processes, and epigenetics. The[illegible] affect[illegible] variety of malignant characteristics by e[illegible]rting antitu[illegible]or or tumor-promoting functions.[26–2[illegible]] Therefore, in-depth studies on lncRNAs in OS may h[illegible]lp to i[illegible]ntify the targets for confirmatory diagnosis and [illegible]ancer therapies. However, studies on lncRNAs [illegible] huma[illegible] OS are limited; therefore, the expres[illegible]n pro[illegible] and functions of cancer-related lncRNAs in [illegible]S require further study. In the present study, the detail[illegible] roles of CCDC144NL-AS1 in OS cells and the underlying mechanisms involved in modulating its malignant characteristics were comprehensively explored. Our results highlight the significance of CCDC144NL-AS1 in OS progression and may contribute toward the development of effective therapies.

CCDC144NL-AS1 is highly expressed in gastric cancer and is associated with poor clinical outcomes.[20] CCDC144NL-AS1 plays an oncogenic role in gastric cancer by regulating multiple tumor behaviors.[20] However, the expression profile and detailed roles of CCDC144NL-AS1 in OS remain largely ambiguous. The results of the current study showed that CCDC144NL-AS1 is overexpressed in OS tissues and cell lines. Furthermore, patients with OS who exhibited high CCDC144NL-AS1 expression had shorter overall survival than those who exhibited low CCDC144NL-AS1 expression. A series of functional assays were performed to analyze the behavioral changes in OS cells after CCDC144NL-AS1 silencing. Interference of CCDC144NL-AS1 expression clearly reduced OS cell proliferation, migration, and invasion and promoted apoptosis in vitro. Additionally, CCDC144NL-AS1 knockdown suppressed OS tumor growth in vivo.

Next, the molecular mechanisms underlying CCDC144NL-AS1-mediated regulation of aggressive OS cells were studied in detail. Many studies have confirmed that lncRNAs function as ceRNAs or molecular sponges to regulate tumorigenesis and tumor development.[29–31] lncRNAs

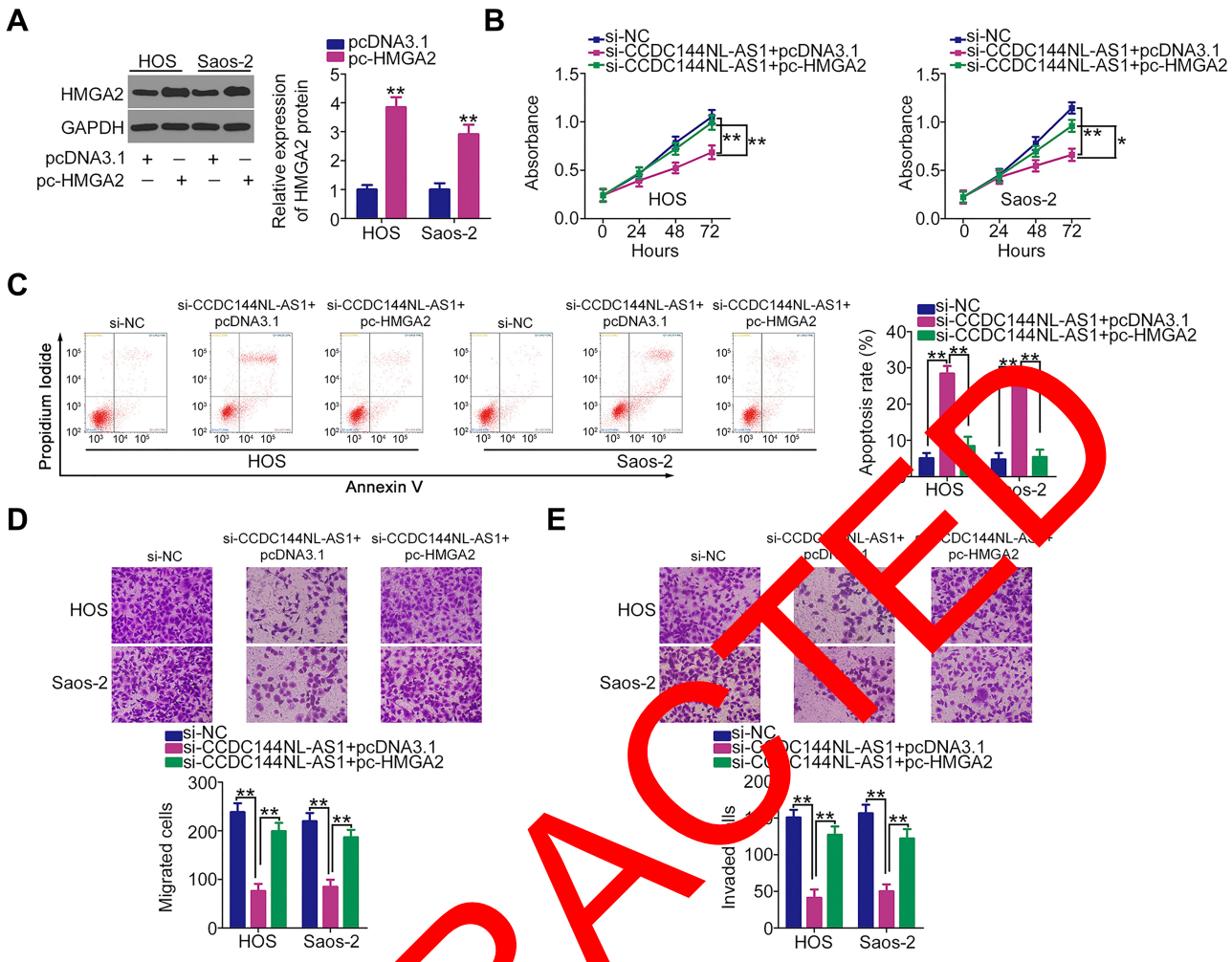

Figure 6 Effects of long noncoding RNA DCST1 antisense RNA (CCDC144NL-AS1) downregulation on the proliferation, apoptosis, migration, and invasion of HOS and Saos-2 cells are largely reversed by restoring high-mobility group AT-hook 2 (HMGA2) expression. (**A**) Western blotting was conducted to determine HMGA2 protein expression in pc-HMGA2-transfected or pcDNA3.1-transfected HOS and Saos-2 cells. (**B**–**E**) CCDC144NL-AS1-depleted HOS and Saos-2 cells were treated with pc-HMGA2 or pcDNA3.1 plasmids and subjected to cell proliferation, apoptosis, migration, and invasion analyses using the Cell Counting Kit 8 (CCK-8) assay, flow cytometric analysis, and Transwell migration and invasion assays, respectively. *P < 0.05 and **P < 0.01.

can competitively bind to miRNAs via miRNA response elements and subsequently increase target mRNA expression.[32] In this study, CCDC144NL-AS1 was mostly distributed in the cell cytoplasm, which provided a theoretical foundation for the ceRNA hypothesis. Through bioinformatics analysis, miR-490-3p was predicted as the target miRNA of CCDC144NL-AS1, which was subsequently validated using luciferase reporter and RIP assays. Additionally, miR-490-3p was shown to be expressed at low levels in OS tissues and showed an inverse correlation with CCDC144NL-AS1 expression. Furthermore, we demonstrated via RT-qPCR analysis that a decrease in CCDC144NL-AS1 expression resulted in a notable upregulation of miR-490-3p expression in OS cells.

HMGA2 was previously reported to be a direct target of miR-490-3p in OS cells,[21] which was experimentally verified in our study. RT-qPCR and Western blotting were used to measure HMGA2 expression in OS cells to elucidate the correlation between CCDC144NL-AS1 and HMGA2 expression. These results showed that the mRNA and protein levels of HMGA2 were decreased in OS cells after CCDC144NL-AS1 depletion, demonstrating that HMGA2 is positively modulated by CCDC144NL-AS1. Further rescue experiments showed that CCDC144NL-AS1 regulates HMGA2 expression in OS by functioning as a sponge for miR-490-3p. Finally, an RIP assay was used to confirm the coexistence of CCDC144NL-AS1, miR-490-3p, and HMGA2 in an RNA-induced silencing complex. In short, our results demonstrate a ceRNA model in OS involving CCDC144NL-AS1, miR-490-3p, and HMGA2.

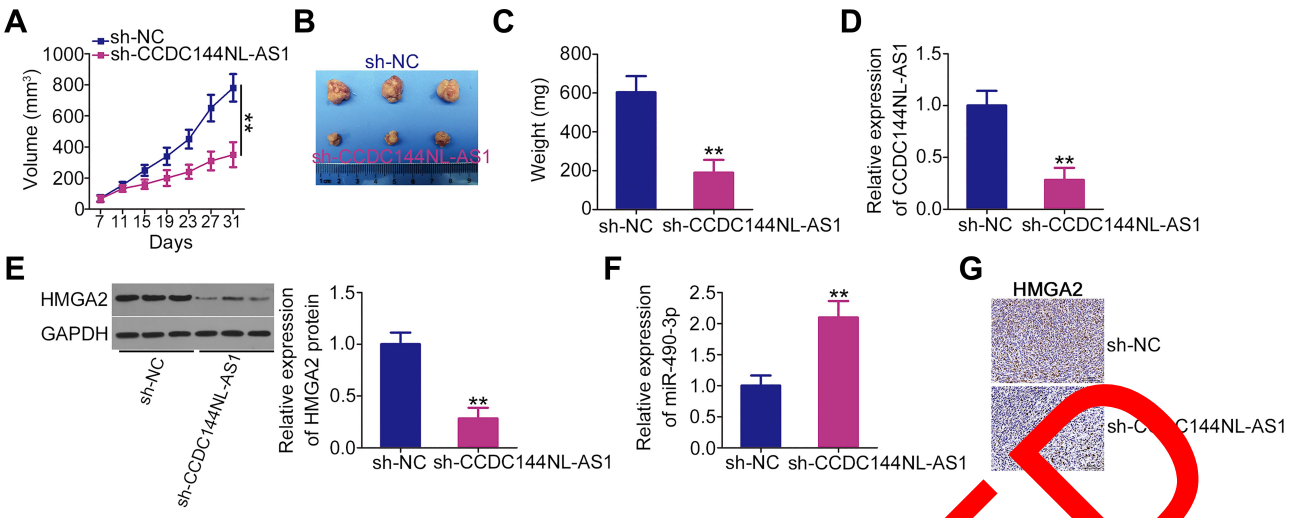

Figure 7 Downregulation of long noncoding RNA DCST1 antisense RNA 1 (CCDC144NL-AS1) impairs osteosarcoma (OS) tumor growth in vivo. (**A**) HOS cells stably expressing sh-CCDC144NL-AS1 or sh-NC via lentiviral infection were subcutaneously injected into nude mice. The volume of the tumor xenografts was recorded every 4 days and a growth curve of tumor xenografts was generated. (**B**) At 31 days following cell injection, all mice were euthanized and tumor xenografts were resected and imaged. (**C**) The weight of the tumor xenografts collected from the sh-CCDC144NL-AS1 and sh-NC groups. (**D** and **E**) Expression of CCDC144NL-AS1 and high-mobility group AT-hook 2 (HMGA2) protein in tumor xenografts was detected using reverse transcription quantitative polymerase chain reaction (RT-qPCR) and Western blotting, respectively. (**F**) RT-qPCR was used to measure miR-490-3p expression in tumor xenografts. (**G**) Immunohistochemical (IHC) analysis was conducted to detect HMGA2 expression in tumor xenografts. **P < 0.01.

miR-490-3p is downregulated in OS[21,33] and presents an obvious correlation with distant metastasis, advanced clinical stage, poor overall survival, and relapse-free survival.[33] Further, it functions as a cancer-inhibiting miRNA by direct targeting HMGA2.[21] HMGA2, a member of the high-mobility group A protein family, is highly expressed in a variety of human cancers, including OS.[22,23] HMGA2 performs pro-oncogenic activities in OS and drives OS genesis and progression.[22,23] Consistent with this result, we found that HMGA2 was overexpressed in OS tissues than in matched adjacent normal tissues. Furthermore, miR-490-3p inhibition or HMGA2 reintroduction partially abolished the suppressive effect of CCDC144NL-AS1 silencing on OS malignant characteristics. These results demonstrate that CCDC144NL-AS1 plays carcinogenic roles in OS cells by acting as a ceRNA to regulate the miR-490-3p/HMGA2 axis.

One miRNA may have multiple direct target genes. In our study, we only identified HMGA2 as the direct target of miR-490-3p in OS. This is a limitation of our study. In the near further, more mechanistic studies will be implemented to identify more direct targets of miR-490-3p in OS.

Conclusion

CCDC144NL-AS1 promotes the initiation and progression of OS by sponging miR-490-3p and increasing HMGA2 expression. Our findings suggest that further research into the CCDC144NL-AS1/miR-490-3p/HMGA2 pathway will provide useful information for OS diagnosis, prognosis, and therapy.

Funding

This study was supported by the Guangxi Natural Science Foundation Youth Science Fund Project (GXNSFBA138019 and 2020GXNSFBA159016), Self-funded research project of Guangxi Health Commission (Z20170424) and Science and Technology Base and Talent Project in Qingxiu District, Nanning City (2020068).

Disclosure

The authors report no conflicts of interest in this work.

References

1. Cortini M, Avnet S, Baldini N. Mesenchymal stroma: role in osteosarcoma progression. *Cancer Lett*. 2017;405:90–99. doi:10.1016/j.canlet.2017.07.024
2. Siegel RL, Miller KD, Jemal A. Cancer statistics, 2015. *CA Cancer J Clin*. 2015;65(1):5–29.
3. Klein MJ, Siegal GP. Osteosarcoma: anatomic and histologic variants. *Am J Clin Pathol*. 2006;125(4):555–581. doi:10.1309/UC6KQHLD9LV2KENN
4. Zhang Y, Yang J, Zhao N, et al. Progress in the chemotherapeutic treatment of osteosarcoma. *Oncol Lett*. 2018;16(5):6228–6237.
5. Lindsey BA, Markel JE, Kleinerman ES. Osteosarcoma overview. *Rheumatol Ther*. 2017;4(1):25–43. doi:10.1007/s40744-016-0050-2
6. Jeys LM, Thorne CJ, Parry M, Gaston CL, Sumathi VP, Grimer JR. A novel system for the surgical staging of primary high-grade osteosarcoma: the birmingham classification. *Clin Orthop Relat Res*. 2017;475(3):842–850. doi:10.1007/s11999-016-4851-y

7. Tsukamoto S, Errani C, Angelini A, Mavrogenis AF. Current treatment considerations for osteosarcoma metastatic at presentation. *Orthopedics*. 2020;1–14.
8. Kung JT, Colognori D, Lee JT. Long noncoding RNAs: past, present, and future. *Genetics*. 2013;193(3):651–669. doi:10.1534/genetics.112.146704
9. Bhan A, Soleimani M, Mandal SS. Long noncoding RNA and cancer: a new paradigm. *Cancer Res*. 2017;77(15):3965–3981. doi:10.1158/0008-5472.CAN-16-2634
10. Peng WX, Koirala P, Mo YY. LncRNA-mediated regulation of cell signaling in cancer. *Oncogene*. 2017;36(41):5661–5667. doi:10.1038/onc.2017.184
11. Zhang Y, Pu Y, Wang J, Li Z, Wang H. Research progress regarding the role of long non-coding RNAs in osteosarcoma. *Oncol Lett*. 2020;20(3):2606–2612. doi:10.3892/ol.2020.11807
12. Xu S, Gong Y, Yin Y, Xing H, Zhang N. The multiple function of long noncoding RNAs in osteosarcoma progression, drug resistance and prognosis. *Biomed Pharmacother*. 2020;127:110141. doi:10.1016/j.biopha.2020.110141
13. Iorio MV, Croce CM. MicroRNA dysregulation in cancer: diagnostics, monitoring and therapeutics: a comprehensive review. . *EMBO Mol Med*. 2017;9(6):852. doi:10.15252/emmm.201707779
14. He L, Hannon GJ. MicroRNAs: small RNAs with a big role in gene regulation. *Nat Rev Genet*. 2004;5(7):522–531. doi:10.1038/nrg1379
15. Otoukesh B, Abbasi M, Gorgani HO, et al. MicroRNAs signatures, bioinformatics analysis of miRNAs, miRNA mimics and antagonists, and miRNA therapeutics in osteosarcoma. *Cancer Cell Int*. 2020;20:254.
16. Jamali Z, Taheri-Anganeh M, Shabaninejad Z, et al. Autophagy regulation by microRNAs: novel insights into osteosarcoma therapy. *IUBMB Life*. 2020;72(7):1306–1321. doi:10.1002/iub.2277
17. Sasaki R, Osaki M, Okada F. MicroRNA-based diagnosis and treatment of metastatic human osteosarcoma. *Cancers*. 2019;11(4):553. doi:10.3390/cancers11040553
18. Kim YH, Goh TS, Lee CS, et al. Prognostic value of microRNAs in osteosarcoma: a meta-analysis. *Oncotarget*. 2017;8(5):8726–8736. doi:10.18632/oncotarget.14429
19. Abdollahzadeh R, Daraei A, Mansoori Y, Sepahvand M, Amoli MM, Tavakkoly-Bazzaz J. Competing endogenous RNA (ceRNA) cross talk and language in ceRNA regulatory network: a new look at hallmarks of breast cancer. *J Cell Physiol*. 2019;234(7):10080–10100. doi:10.1002/jcp.27811
20. Fan H, Ge Y, Ma X, et al. Long non-coding RNA CCDC144NL-AS1 sponges miR-143-3p and regulates PIK3CA/AKT/mTOR pathway by acting as a competing endogenous RNA in gastric cancer. *Cell Death Dis*. 2020;11(7):521. doi:10.1038/s41419-020-02740-2
21. Liu W, Xu G, Liu H, Li T. MicroRNA-490-3p regulates cell proliferation and apoptosis by targeting HMGA2 in osteosarcoma. *FEBS Lett*. 2015;589(20 Pt A):3148–3153. doi:10.1016/j.febslet.2015.08.034
22. Xia Q, Ni J, Huang J, Pan B, Yan M, Li W. [Suppression of miR-30a/HMGA2-mediated autophagy in osteosarcoma cells impacts chemotherapeutics-induced apoptosis]. *Zhong Nan Da Xue Xue Bao Yi Xue Ban*. 2019;44(7):757–766. Chinese.
23. He QY, Wang GC, Zhang H, et al. miR-106a-5p suppresses the proliferation, migration, and invasion of osteosarcoma cells by targeting HMGA2. *DNA Cell Biol*. 2016;35(9):506–520. doi:10.1089/dna.2015.3121
24. Xia P, Gu R, Zhang W, Sun YF. lncRNA CEBPA-AS1 overexpression inhibits proliferation and migration and stimulates apoptosis of OS cells via notch signaling. *Mol Ther Nucleic Acids*. 2020;19:1470–1481. doi:10.1016/j.omtn.2019.10.017
25. Zhang L, Zhao G, Ji S, Yuan Q, Zhou H. Downregulated long non-coding RNA MSC-AS1 inhibits osteosarcoma progression and increases sensitivity to cisplatin by binding microRNA-142. *Med Sci Monit*. 2020;26:e921594.
26. Yang C, Cai X, Yu M, et al. Long noncoding RNA OR3A4 promotes the proliferation and invasion of osteosarcoma cells by sponging miR-1227-5p. *J Bone Oncol*. 2020;21:100278. doi:10.1016/j.jbo.2020.100278
27. Chen L, Wang J, Li W, Zhao W, Tian LF. lncRNA MEG3 inhibits proliferation and promotes apoptosis of osteosarcoma cells through regulating Notch signaling pathway. *Eur Rev Med Pharmacol Sci*. 2020;24(2):581–590.
28. Zha Z, Han Q, Liu W, Huo J. lncRNA GAS8-AS1 downregulates lncRNA UCA1 to inhibit osteosarcoma cell migration and invasion. *J Orthop Surg Res*. 2020;15(1):38. doi:10.1186/s13018-020-1550-x
29. Credendino SC, Bellone ML, Lewin N, et al. A ceRNA circuitry involving the long noncoding RNA Klhl14-AS, Pax8, and Bcl2 drives thyroid carcinogenesis. *Cancer Res*. 2019;79(22):5746–5757. doi:10.1158/0008-5472.CAN-19-0039
30. Sun C, Hu X. lncRNA SNHG6 functions as a ceRNA to up-regulate c-Myc expression via sponging let-7c-5p in hepatocellular carcinoma. *Biochem Biophys Res Commun*. 2019;519(4):901–908. doi:10.1016/j.bbrc.2019.09.091
31. Tong H, Zhuang X, Cai J, et al. Long noncoding RNA ZFAS1 promotes progression of papillary thyroid carcinoma by sponging miR-590-3p and upregulating HMGA2 expression. *Onco Targets Ther*. 2019;12:7501–7512. doi:10.2147/OTT.S209138
32. Wang L, Cho KB, Li Y, Tao G, Xie Z, Guo B. Long noncoding RNA (lncRNA)-mediated competing endogenous RNA networks provide novel potential biomarkers and therapeutic targets for colorectal cancer. *Int J Mol Sci*. 2019;20(22).
33. Tang B, Liu C, Zhang QM, Ni M. Decreased expression of miR-490-3p in osteosarcoma and its clinical significance. *Eur Rev Med Pharmacol Sci*. 2017;21(2):246–251.